Journal of Geochemical Exploration 190 (2018) 26–38

Contents lists available at ScienceDirect

Journal of Geochemical Exploration

journal homepage: www.elsevier.com/locate/gexplo

Northern Puna Plateau-scale survey of Li brine-type deposits in the Andes of NW Argentina

R. Lucrecia López Steinmetz[a,b,*], Stefano Salvi[c], M. Gabriela García[d], Y. Peralta Arnold[b,e], Didier Béziat[c], Gabriela Franco[b], Ornela Constantini[b], Francisco E. Córdoba[b,e], Pablo J. Caffe[b,e]

[a] Instituto de Geología y Minería, Universidad Nacional de Jujuy, Av. Bolivia 1661, S.S. de Jujuy 4600, Argentina
[b] Instituto de Ecorregiones Andinas (INECOA), Universidad Nacional de Jujuy - CONICET, S.S. de Jujuy 4600, Argentina
[c] Université de Toulouse, CNRS, GET, IRD, OMP, 14 Av. Edouard Belin, Toulouse 31400, France
[d] CICTERRA-CONICET-Universidad Nacional de Córdoba, Córdoba 5016, Argentina
[e] Facultad de Ingeniería, Universidad Nacional de Jujuy, Argentina

ARTICLE INFO

Keywords:
Lithium
Salars
Central Andes
Altiplano-Puna Plateau
Hydrochemistry

ABSTRACT

Salars of the Andean Plateau in the Central Andes are the largest lithium deposits on Earth. The most notorious are the Chilean Salar de Atacama, and Uyuni in the Bolivian Altiplano. Despite the relevance of the region concerning the lithium resources, there is still scarce scientific literature on the hydrochemistry of lithium deposits in the Argentine portion of the Andean Plateau. In this article we present new hydrochemical data from the first regional-scale reconnaissance exploration of the four major salars in the northernmost Argentine Andes. Data revealed that brines in the studied salars are characterized by mean Li concentrations ranging between 82 and 1014 mg L^{-1}, and mean Li:Mg ratios from 0.92 to 0.54. The size of the study salars becomes a potential limitation for the whole Li resources in comparison with the giant Atacama and Uyuni. Nonetheless, when considering the Li grade and the Li:Mg ratio of brines, the Northern Puna salars turn out to be very remarkable lithium prospects. Data emerged from this survey represent a valuable tool for: 1) private investment projects by defining Li mining targets, 2) for the administration of natural resources and the definition of the State's politics, and 3) for scientific purposes, especially in investigations meant to better understand the processes involved in the formation of Li brine deposits, salars, and endorheic basins.

1. Introduction

Salars of the Central Andes are the largest lithium deposits on Earth (Warren, 2010; Houston et al., 2011; Kesler et al., 2012; Munk et al., 2016). Particularly, the largest global resources concentrate in numerous internally drained basins of Chile, Bolivia and Argentina, where the lithium (Li) extraction has already become an important source of income in these South American countries. The Andean salars of Uyuni in Bolivia and Atacama in Chile (Fig. 1) contain the most important known Li resources in the world (Moraga et al., 1974; Gruber and Medina, 2010; Mohr et al., 2010; Kunasz, 2006; Kesler et al., 2012; Munk et al., 2016).

Uyuni is a spectacularly giant salar and with a surface of > 10,500 km^2 it is the largest salt pan of the Andes and on Earth (Risacher and Fritz, 1991; Kesler et al., 2012). This salt pan is located in the Altiplano at 3663 m a.s.l. (Fig. 1). The mean Li content in the near-surface brines of Uyuni ranges from 316 to 602 mg L^{-1} and the Li concentration pattern across the salar increases towards the south (Ericksen et al., 1976; Ericksen and Salas, 1977; Rettig et al., 1980; Risacher and Fritz, 1991; Schmidt, 2010). The estimated Li resources of Uyuni are over 10.20 Mt., which represent ~12 times the estimated resources of Greenbushes in Australia, the world famous Li pegmatite deposit (Kesler et al., 2012).

Although Uyuni is probably the most important Li resources worldwide, this salar is not in production yet. Much of the Li being produced globally at present is obtained from the Salar de Atacama. With estimated resources reaching 6.30 Mt., Atacama is thus the most important Li mine in the world (Moraga et al., 1974; Ide and Kunasz, 1989; Kunasz, 2006; Lowenstein and Risacher, 2009; Gruber and Medina, 2010; Mohr et al., 2010; Kesler et al., 2012; COCHILCO, 2013).

The Salar de Atacama (Fig. 1) is a 3000 km^2 salt pan located at 2300 m a.s.l., whose halite nucleus spreads 1100 km^2 and ~1000 m depth (Moraga et al., 1974; Stoertz and Ericksen, 1974; Bevacqua, 1992; Alonso and Risacher, 1996; Carmona et al., 2000; Boschetti et al., 2007; Jordan et al., 2007; Boutt et al., 2016; Corenthal et al., 2016). The average Li concentration of Atacama is ~1400 mg L^{-1}, ranging

* Corresponding author at: Instituto de Geología y Minería, Universidad Nacional de Jujuy, Av. Bolivia 1661, S.S. de Jujuy, 4600, Argentina.
E-mail address: lucrecialopezsteinmetz@hotmail.com (R. Lucrecia López Steinmetz).

https://doi.org/10.1016/j.gexplo.2018.02.013
Received 6 June 2017; Received in revised form 13 February 2018; Accepted 25 February 2018
Available online 01 March 2018
0375-6742/

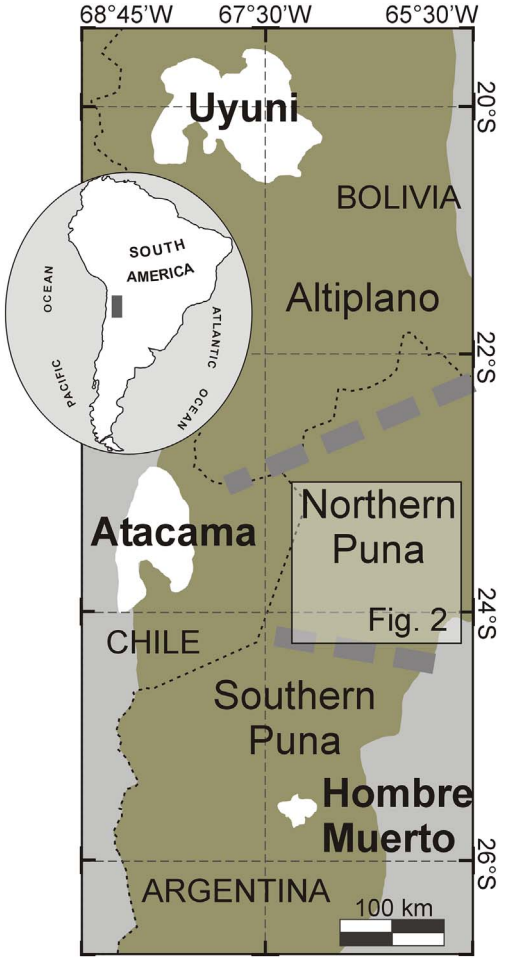

Fig. 1. Map of the Andean Plateau (dark green area), showing the location of the Salar de Atacama, Uyuni and Hombre Muerto (white areas). Thick dashed grey lines indicate the internal Plateau boundaries between the Bolivian Altiplano, the Argentinean Northern and Southern Puna (Alonso et al., 1984). There are many other salars in the Chilean Desierto de Atacama, in the Bolivian Altiplano and in the Argentinean Puna Plateau that are not shown in this map. (For interpretation of the references to colour in this figure legend, the reader is referred to the web version of this article.)

between 1000 and 6400 mg L^{-1} (Moraga et al., 1974; Ide and Kunasz, 1989; Kunasz, 2006), representing the maximum Li concentration in a brine-type deposit reported to date worldwide. The Li concentration pattern across the Salar de Atacama is well known: five concentric Li grade zones were defined, with the higher Li grade zone located in the southern part of the salar (Ide and Kunasz, 1989).

In the Argentine Puna region, in the southernmost part of the Andean Plateau (Fig. 1), there are also some remarkable Li prospects. The most prominent is the Salar de Hombre Muerto (Fig. 1), which became the first Li mine operating in Argentina since the 90's (Kesler et al., 2012; Fornillo et al., 2015). Hombre Muerto comprises a 300 km^2 salt pan placed at 3970 m a.s.l., with estimated Li resources of 0.80 Mt., and mean Li contents of ~520 mg L^{-1}; the concentration pattern across the salar increases towards the south (Garrett, 2004; Kesler et al., 2012; Godfrey et al., 2013).

As mentioned, the Li resources of salars in the Chilean Desierto de Atacama and the Bolivian Altiplano are largely known (Ericksen and Salas, 1977; Ide and Kunasz, 1989; Risacher and Fritz, 1991; Alonso and Risacher, 1996; Risacher et al., 1999; Carmona et al., 2000; Risacher et al., 2003; Kunasz, 2006; Risacher and Fritz, 2009). On the contrary, and despite the relevance of this strategic mineral resource and the outstanding prospect of the Andean salars, there are still scarce scientific works on the hydrochemistry of Li deposits in the Argentinean Puna (Fig. 1). This region is becoming an increasing focus of exploration activity. Most of the available information of Puna salars is based on reports provided by mining companies and regional data reported in a number of scientific papers (Yaksic and Tilton, 2009; Gruber and Medina, 2010; King, 2010; Houston et al., 2011; Fornillo et al., 2015; Munk et al., 2016). On the contrary, local works aiming to characterize the hydrochemistry of Li deposits in this Andean region are restricted to the Salar de Hombre Muerto (Godfrey et al., 2013; Fig. 1) and the Salar de Centenario-Ratones (Orberger et al., 2015) in the Southern Puna, and the Guayatayoc playa lake in the Northern Puna (López Steinmetz, 2017; Fig. 2). There are still many other salars in the Puna region that are promising Li prospects, and that – to date – were not object of scientific surveys, even of a reconnaissance nature. For instance, in the Northern Puna little is known about the hydrochemistry of the Cauchari and the Salinas Grandes salt pans, whereas the Salar de Jama remains completely unexplored (Fig. 2).

In this work we report the results of a regional Li exploration campaign covering an area of 9000 km^2 in the endorheic Northern Puna (Fig. 2) that includes the four major salars which represent promising Li prospects. The major chemical composition and Li content of brine samples collected from the Salar de Jama, Olaroz, Cauchari and Salinas Grandes are analysed in order to contribute to the knowledge of the Andean salars hydrochemistry from a regional perspective. This research is the first scientific report on Li resources in the Northern Puna Plateau, and, along with the information previously reported by López Steinmetz (2017), completes the first broad survey of Li-bearing salars on the northern Argentine Plateau. We finally propose to discuss the Li resource perspectives of the Northern Puna region in the context of the most notorious Andean prospects.

2. The study area

The salars analysed in this study are all set in the endorheic Northern Puna region (Fig. 2). The Salar de Jama is the smallest one, and is located on the Argentina-Chile border, at the foothills of the Jama volcano. Eastward, the Salar de Olaroz and Cauchari occupy the same north-south elongate orographic depression, superficially detached one from the other by prograding alluvial fans (the composite Archibarca alluvial cone). Finally, the Salinas Grandes covers the easternmost reaches of the lower Northern Puna, limiting to the north with the Guayatayoc salar basin.

There is an altitudinal gradient across the Northern Puna, which determines that western salars are placed at higher altitude than those located to east (Fig. 2). These four salars extend between 23° and 24°S. Northward, the endorheic basins of the Northern Puna are characterized by the presence of lakes that only occasionally dry out (e.g., Laguna de Pozuelos, McGlue et al., 2012; Laguna de Pululos, Lupo et al., 2006).

Orographic depressions that host salars are defined by north-south trending ranges formed during Andean thrusting events. These ranges expose the basement, which consist of Lower to Middle Ordovician (Santa Victoria Group, Turner, 1960a, 1960b) and Precambrian - Eocambrian (Puncoviscana Formation, Turner, 1960a, 1960b) metasedimentary rocks in the Puna Plateau and the Eastern Cordillera, respectively. The latter unit, together with Upper Cambrian sedimentary rocks (Meson Group, Turner, 1960a, 1960b) are only present along the eastern border of the study area (Fig. 2). Middle to Upper Ordovician peraluminous, plutonic complexes and Jurassic to Cretaceous alkaline granites (Méndez et al., 1973; Zappettini, 1989; Coira et al., 1999; Cristiani et al., 1999; Kirschbaum et al., 2006) are widely distributed in ranges along the western side of the Salinas Grandes and, in a lesser extent, along the eastern margin of the Salar de Olaroz (Fig. 2).

Cretaceous to Paleocene rift-related sedimentary rocks (Salta Group, Turner, 1959) frequently crop out overlain by Upper Eocene to Upper Miocene synorogenic deposits (Turner, 1972; Schwab, 1973; Schwab and Lippolt, 1974; Arias and Viera, 1982; Seggiaro, 2013). These units

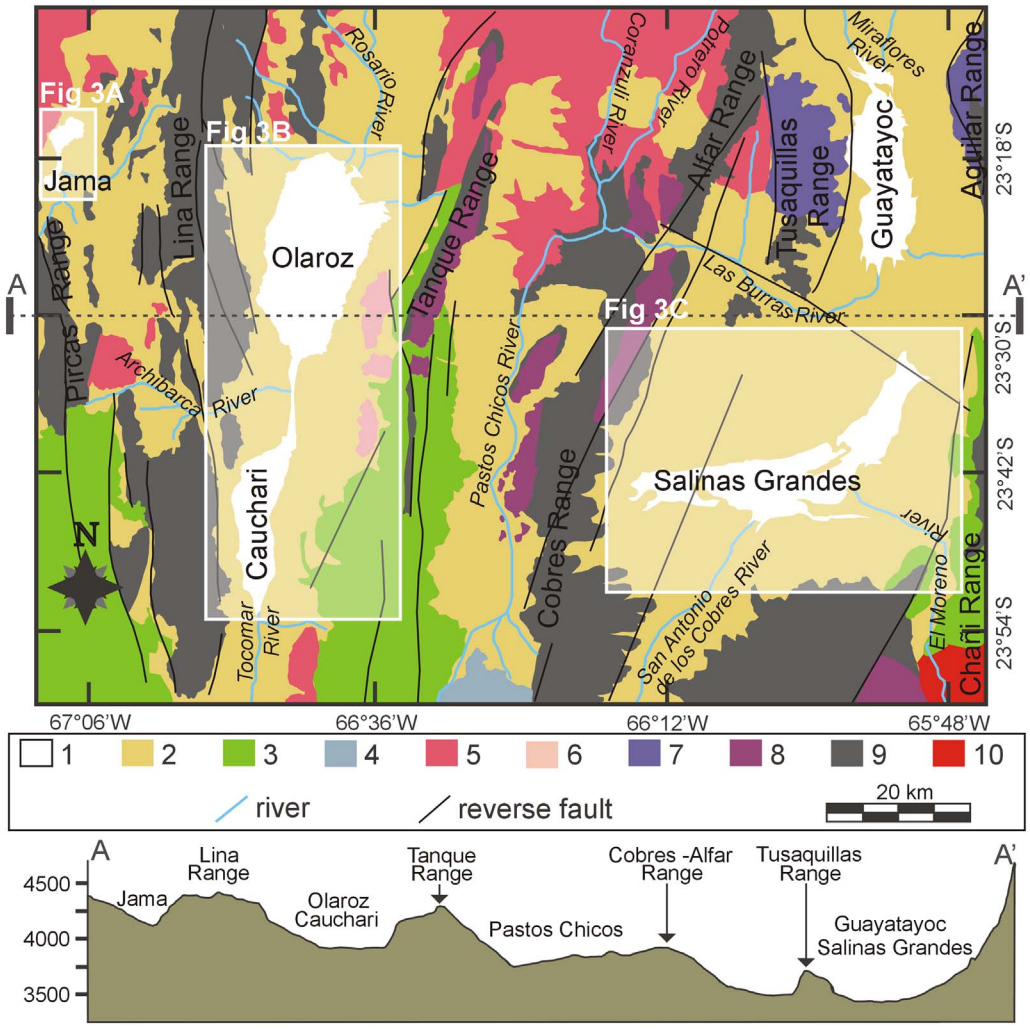

Fig. 2. Simplified geologic map of the Northern Puna Plateau between 23°06′S and 23°56′S, modified from González et al. (2000), Coira et al. (2004), and Seggiaro (2013). The map shows the location of the Northern Puna's salars. A–A′ is the altitudinal transect of the Northern Puna Plateau at 23°30′S. Lithological legend: 1) modern salar; 2) Quaternary alluvial deposits, including piedmonts, alluvial fans and alluvial plains; 3) sedimentary units including the Cretaceous-Paleocene rift related and the Upper Eocene to Upper Miocene synorogenic deposits; 4) Plio-Pleistocene ignimbrite; 5) Miocene-Pliocene ignimbrite; 6) Miocene dacite; 7) Jurassic-Cretaceous granite; 8) Ordovician granite; 9) Ordovician metasedimentary basement of the Northern Puna; 10) Precambrian-Eocambrian metasedimentary basement of the Eastern Cordillera and Upper Cambrian sedimentary units.

are widespread in the southern portions of the Tanque and Pircas ranges, and in the Alta range, in the southern border of the Salinas Grandes.

Paleogene to Lower Miocene continental red beds (Log Log, Vizcachera and Peña Colorada formations; see Coira et al., 2004; Seggiaro, 2013; and references therein) were deposited afterwards in a broken foreland environment (e.g., del Papa et al., 2013), Fluviatile to lacustrine deposits intercalated with air fall tuffs and pyroclastic flow deposits (Tiomayo, Trincheras and Pastos Chicos formations) characterize the Middle to Upper Miocene (16 to 10 Ma) sedimentary/volcaniclastic record (Schwab and Lippolt, 1974; Coira et al., 2004). Towards the Upper Miocene-Pliocene transition similar sedimentary sequences (Loma Blanca/Sijes Formation; Alonso, 1986) locally involved deposition of evaporite facies (Olaroz-Coranzulí).

Large areas of the Northern Puna are covered by Upper Miocene-Pliocene and Pleistocene ignimbrites, dacite to rhyolite lavas and subvolcanic intrusions, and mafic andesite volcanic centres (Coira et al., 1993; Seggiaro, 1994; Coira et al., 2004; Soler et al., 2007; Seggiaro, 2013; Maro and Caffe, 2016; and references therein). Quaternary alluvial fan deposits extend between the foot of the mountains and the flat areas, which are covered by fine-grained sediments and salt pans. Salar mining in the Northern Puna was traditionally related to the extraction of halite and ulexite from these salt pans, while Li mining started recently (2014), the Salar de Olaroz and Cauchari being the only active brine prospects (Fornillo et al., 2015).

The environmental conditions that prevail in these high-altitude endorheic basins are typically extreme, with low effective precipitation and wide temperature fluctuations. Thus, rainfall is markedly seasonal, with ~70% of the yearly total falling during the austral summer (December–March), while the dry season spans over the rest of the year. High rates of evaporation and low annual rainfall, averaging 150–400 mm and increasing from SW to NE, are responsible for a negative water balance. As a consequence, fluvial systems mainly consist of ephemeral streams. Despite most tributaries infiltrate before reaching the salars, some major fluvial collectors feed the systems over the year (Fig. 2). In addition, groundwater discharge probably represents an important source of water to the salar systems (Peralta Arnold et al., 2017).

3. Methods

For the Li reconnaissance exploration and hydrochemical assessment of the Northern Puna salars, residual brines were sampled across the Salar de Jama (JA), Olaroz (OL), Cauchari (CA) and Salinas Grandes (SG, Fig. 3). The detailed location of samples is presented in Table A as electronic Supplementary material. Brine samples were collected and analysed during the austral spring 2010 (from September until December). Samples were collected at 40 to 90 cm depth in pits dug in salars, except for samples JA10, OL10, CA1, CA2 and SG10 that were collected from brine pools. Samples were stored in pre-cleaned polyethylene bottles and preserved refrigerated during transport.

Brine samples were analysed at the Agua de los Andes S. A. laboratory. Analytical results are summarized in Table 1. Physicochemical parameters such as pH and electrical conductivity were determined

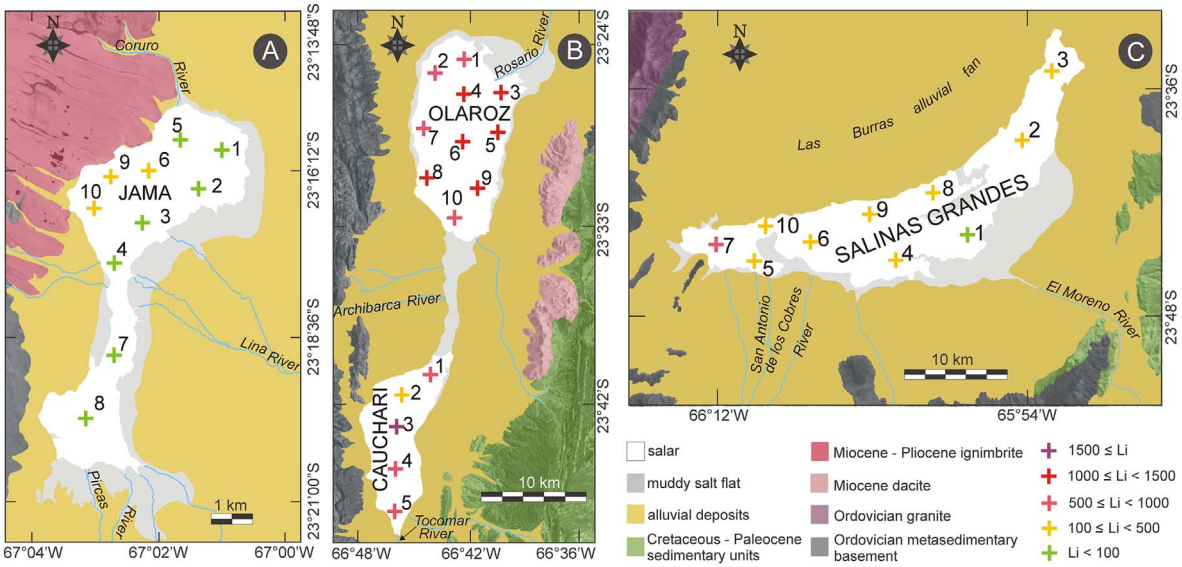

Fig. 3. Maps showing the location of shallow brine sampling points (numbered crosses) and Li grade zones in the Salar de Jama (A), Olaroz, Cauchari (B) and Salinas Grandes (C). Brine Li concentrations are in mg L^{-1}. Precise latitude and longitude of the samples are given in Table A of the electronic Supplementary material.

with a Hanna HI2314 multi-range conductivity meter. The salinity of samples is expressed as the total dissolved solids (TDS). TDS in mg L^{-1} have been obtained by employing a conversion factor of 0.50 on the measured electrical conductivity. The major ion composition was determined following standard recommendations (Clesceri et al., 1998). Calcium (Ca^{2+}) was determined by titration using a 0.01 M EDTA solution, while magnesium (Mg^{2+}) was calculated as the difference between total hardness and calcium concentration. Chloride (Cl^-) was determined by titration using the argentometric method. Sulphate (SO_4^{2-}) was precipitated in an acetic acid medium with $BaCl_2$ and its concentration was determined by turbidimetry. Bicarbonate and carbonate (HCO_3^- and CO_3^{2-}) were determined by titration using a 0.01 N

Table 1
Chemical composition of brines samples collected in the Salar de Jama (JA), Olaroz (OL), Cauchari (CA) and Salinas Grandes (SG).

Sample	pH	mg L^{-1}									
		TDS	Ca^{2+}	Mg^{2+}	Na^+	K^+	Li^+	Cl^-	SO_4^{2-}	$CO_3^{2-} + HCO_3^-$	B
JA1	8.2	7301.82	1780.25	402.30	2004.26	200.58	6.38	2560.43	7009.41	348.60	538.89
JA2	8.2	7421.05	991.35	243.11	2859.81	342.99	11.21	2627.16	4586.61	386.50	3069.90
JA3	8.2	6278.71	130.61	17.29	3523.22	210.43	9.71	6170.13	2051.34	332.10	236.33
JA4	8.7	6188.43	121.78	48.04	3421.86	343.95	1.52	4927.21	2536.63	233.70	492.99
JA5	8.8	6177.76	65.13	46.70	4182.54	296.61	2.26	5868.37	1219.43	262.90	238.54
JA6	8.2	91,054.52	646.66	469.37	60,432.10	4590.64	262.08	97,016.83	14,615.24	286.40	1421.42
JA7	8.2	6187.05	121.69	47.94	3474.84	344.25	1.53	4929.37	2535.17	341.20	492.91
JA8	8.2	6163.70	122.02	47.44	3482.00	343.69	1.57	4930.20	2540.53	344.00	493.71
JA9	8.5	90,269.69	646.67	467.32	60,426.52	3355.90	262.15	97,017.84	14,615.59	281.60	1421.42
JA10	8.7	91,815.96	645.53	491.97	60,436.79	4658.47	261.22	97,016.74	14,615.78	271.50	1421.97
OL1	8.3	157,266.80	583.68	1539.30	112,191.11	5051.43	771.21	181,748.88	9677.98	421.10	2089.58
OL2	8.2	158,318.45	529.21	1980.75	112,190.20	5504.30	967.88	181,002.79	10,222.33	418.60	2089.70
OL3	8.2	155,257.43	526.29	1971.71	107,654.41	6018.97	1006.99	179,626.85	10,191.76	435.00	2301.87
OL4	8.4	156,631.74	480.90	2301.38	107,956.50	7983.73	1206.59	180,836.96	8982.22	328.10	3175.89
OL5	8.1	136,829.08	447.67	2183.36	69,854.56	6562.58	1091.71	175,695.02	10,585.40	343.20	2510.90
OL6	8.1	153,032.24	496.21	2276.19	79,670.03	7870.00	1213.24	187,040.81	10,014.55	366.40	2251.41
OL7	8.2	157,686.26	512.90	1988.32	107,758.99	5178.60	867.53	176,344.59	9856.27	330.90	2422.31
OL8	8.5	160,072.88	536.99	2185.80	107,068.69	5500.58	1093.28	184,987.41	10,202.73	280.10	3036.87
OL9	8.2	159,123.54	447.19	1627.83	112,332.31	6002.77	1061.19	179,090.57	10,658.38	246.70	2799.82
OL10	8.3	144,562.76	597.80	1970.19	71,783.37	6568.89	860.56	181,605.40	10,373.53	265.80	2655.30
CA1	8.6	97,360.60	555.98	1851.41	69,825.60	2976.48	535.39	108,014.40	9060.48	278.60	1336.61
CA2	9.1	92,423.61	763.78	1508.83	58,032.00	2714.40	441.79	102,211.20	14,470.56	355.40	2190.24
CA3	9.3	123,655.57	603.23	1669.64	85,708.80	8593.92	1739.52	130,406.40	11,957.76	489.80	2833.92
CA4	8.3	139,239.69	476.93	1594.08	101,347.20	4769.28	712.80	149,817.60	16,355.52	461.30	2304.29
CA5	7.2	144,418.82	599.18	2103.98	104,515.20	4733.28	872.78	163,886.40	9685.44	623.10	2125.87
SG1	8.0	11,692.52	876.73	115.36	6413.45	693.62	25.12	10,203.36	3982.07	374.50	527.14
SG2	7.1	120,191.96	1306.59	803.13	86,374.71	3324.81	218.33	140,686.30	1746.18	341.80	508.79
SG3	7.1	118,931.11	1461.99	1017.27	84,717.51	3497.69	244.11	141,354.44	1573.50	344.30	542.05
SG4	7.0	120,539.30	1442.32	1130.15	86,816.89	3761.91	269.61	140,265.87	2174.46	338.70	443.92
SG5	7.2	116,328.36	1906.37	1300.67	77,468.50	4521.35	382.08	140,411.83	1908.26	256.10	451.62
SG6	8.0	116,091.60	1471.79	842.91	79,327.30	3650.79	241.16	139,302.24	2387.76	278.30	341.65
SG7	7.1	116,136.09	2119.41	2288.58	67,954.24	8148.89	1018.23	139,071.47	1441.45	230.20	360.93
SG8	8.0	119,366.34	1431.94	923.75	80,246.15	3889.64	246.51	139,796.77	1958.78	351.20	309.48
SG9	8.0	117,527.40	1394.66	1021.96	85,692.72	4668.09	325.45	137,845.93	1900.26	367.60	512.13
SG10	7.7	116,394.57	1787.43	1233.00	77,539.22	5196.13	351.80	137,690.57	1750.81	259.70	469.15

sulfuric acid solution and methyl-orange and phenolphthalein were used as end-point indicators, respectively. Boron (B) was determined by colorimetry using carmine reactive. Sodium (Na^+), potassium (K^+) and lithium (Li^+) were determined by Atomic Emission Spectroscopy. Ion balances were typically lower than 5% in all cases (see the Fig. A of the electronic Supplementary material). Saturation index (SI) was calculated by using PHREEQC 3.3.8, and employing the Pitzer database.

4. Li-bearing salars of the Northern Puna

4.1. The Salar de Jama

Jama is a north-south elongated salt pan located at 4080 m a.s.l. The salar surface is 25 km^2, spreading between 67°02′–67°04′W and 23°15′–23°21′S (Fig. 3A). Main tributaries are the Coruro, Lina and Pircas Rivers. Local lithology involves the Ordovician metasedimentary basement and Miocene-Pliocene ignimbrites (the Mucar, Atana and Toconao ignimbrites), dacite lavas as well as small mafic andesite volcanic centres (the Jama and Archibarca volcanoes). The salar overlies Quaternary alluvial deposits that interdigitate with a muddy salt shoreline along the south-eastern border of the salar.

Jama's brines are alkaline, with pH values ranging between 8.2 and 8.8 (Table 1), and moderately saline, with TDS ranging between 6163 and 91,815 mg L^{-1} (Table 1). According to their major chemical composition, brines are of the Na/Cl^--SO_4^{2-} type, with relatively abundant Ca^{2+} and K^+ (Fig. 4). Major ion concentrations are the highest in the north-western margin of the salar, close to Miocene-Pliocene ignimbrite outcrops.

When the mean ionic concentration of Jama's brines is compared with those of the other Northern Puna salars, the Jama brines result the most dilute (Fig. 5). The concentrations of Na^+ in the Jama's brines show a positive linear correlation with Cl^- concentrations (Fig. 6A) with a mean Na:Cl ratio of 1:1.10, which is close to the 1:1 stoichiometric ratio that characterizes the dissolution of halite. Fig. 6 depicts the variations of SO_4^{2-} with Ca^{2+} (Fig. 6C), Mg^{2+} (Fig. 6E), and

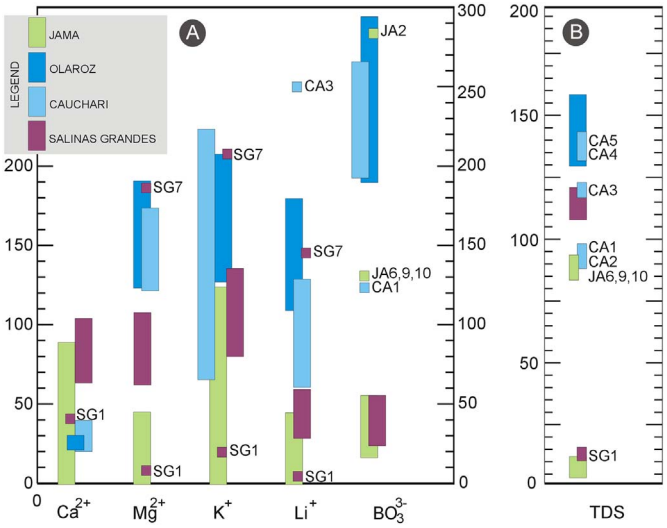

Fig. 5. Comparative concentrations of Ca^{2+}, Mg^{2+}, K^+, Li^+ and BO_3^{3-} (g L^{-1}) (A) and TDS (g L^{-1}). (B) of samples collected from the Salar de Jama (JA), Olaroz (OL), Cauchari (CA) and Salinas Grandes (SG).

$Ca^{2+} + Mg^{2+}$ (Fig. 6F) concentrations in the analysed brines. As seen in these figures, the concentrations of Ca^{2+}, Mg^{2+} and SO_4^{2-} in the Jama's brines show positive linear trends characterized by $SO_4^{2-} > Ca^{2+}$, $SO_4^{2-} > Mg^{2+}$, and $SO_4^{2-} > Ca^{2+} + Mg^{2+}$ ratios, which suggests that the dissolution of Ca-Mg sulphates is not the unique mechanism contributing sulphate ions.

The Li^+ concentration in the Jama's brines ranges between 1.50 and 262 mg L^{-1}, with the highest Li grade zone along the north-western border of the salar (Fig. 3A), and a mean Li^+ concentration being 82 mg L^{-1}. Positive linear trends are observed between the Li^+ concentrations and those of K^+ and Mg^{2+} (Fig. 7A, C); the mean Li:K ratios is 0.18 while the mean Li:Mg ratio is 0.42 (Table 2). Boron

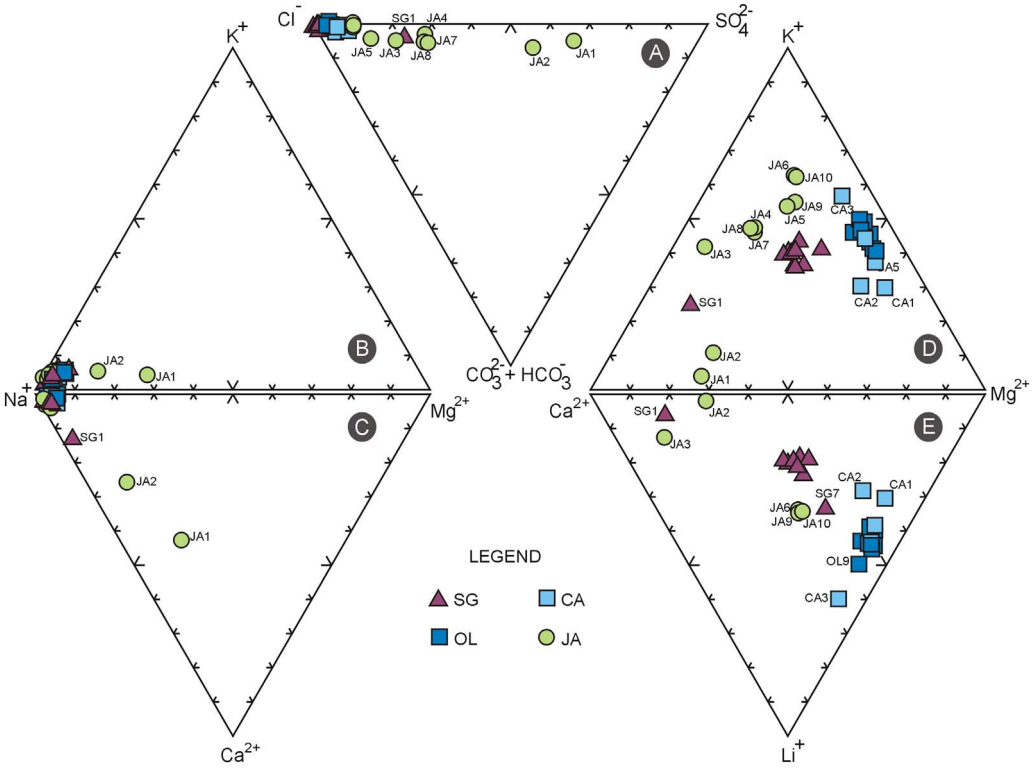

Fig. 4. Ternary diagrams showing the relative ionic concentrations of brines from the Salar de Jama (JA), Olaroz (OL), Cauchari (CA) and Salinas Grandes (SG). Ionic concentrations are expressed in meq L^{-1}.

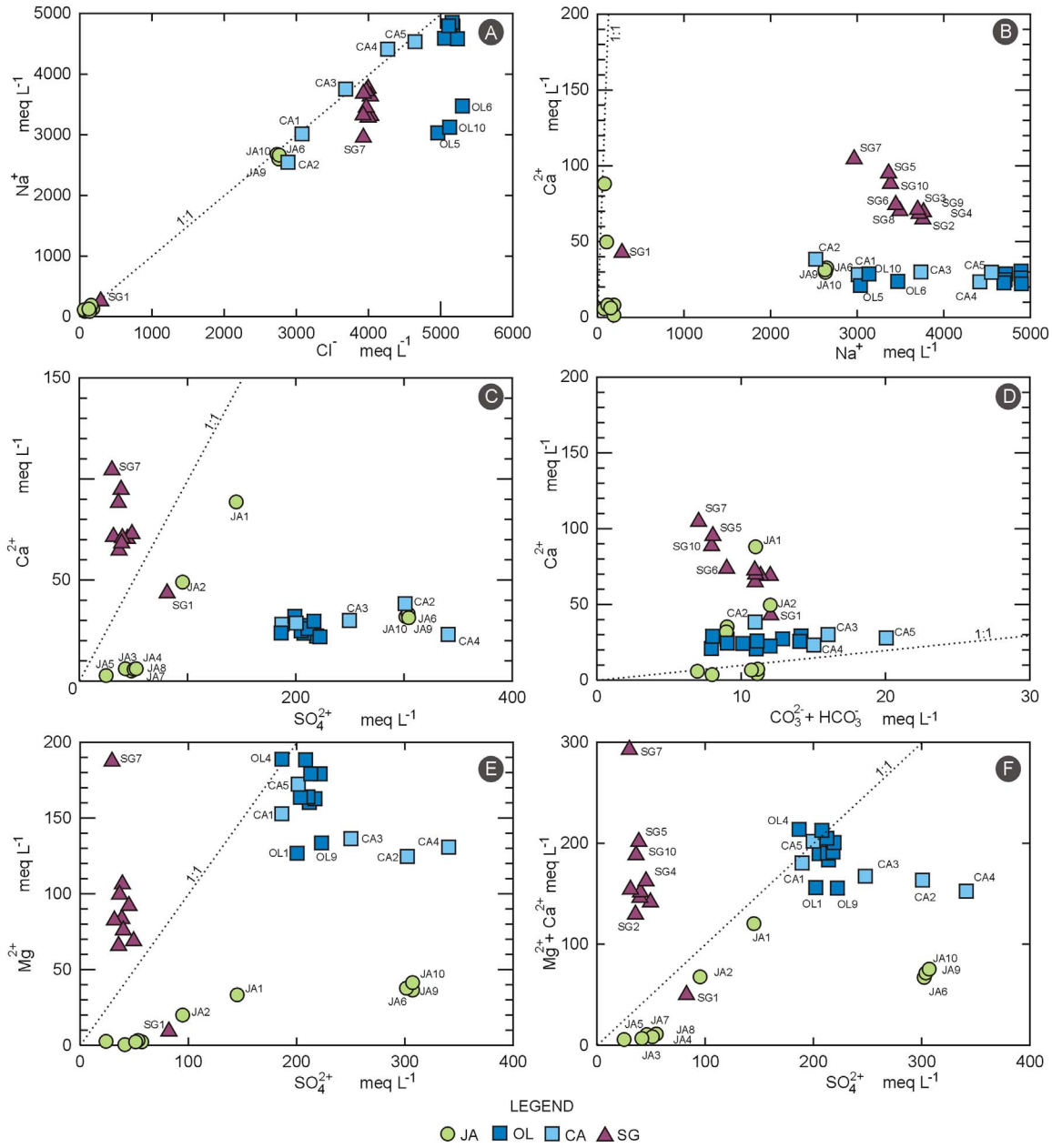

Fig. 6. Scatter diagrams showing the variation of Na^+ versus Cl^- (A), Ca^{2+} versus Na^+ (B), Ca^{2+} versus SO_4^{2-} (C), Ca^{2+} versus $CO_3^{2-} + HCO_3^-$ (D), Mg^{2+} versus SO_4^{2-} (E), and $Mg^{2+} + Ca^{2+}$ versus SO_4^{2-} (F) in the Jama (JA), Olaroz (OL), Cauchari (CA), and Salinas Grandes (SG).

concentrations in these brines range between 236 and 3.07 mg L^{-1}. No linear correlation between Li and B has been observed, being Li < B with the mean Li:B ratio = 0.10 (Fig. 7B).

4.2. The Salar de Olaroz and Cauchari

These two salars are located in a N-S elongated basin at an average altitude of 3903 m a.s.l. The Salar de Olaroz is a 130 km^2 salt pan spanning between 66°39′–66°45′W and 23°24′–23°33′S (Fig. 3B). The northern catchment area includes numerous hydrothermal springs (Peralta Arnold et al., 2017), where the main fluvial collector is the Rosario River that discharges into the north of the salar. The other main tributary to the salar is the Archibarca River that reaches the salt pan from the west. This river forms a huge prograding alluvial fan that dissects the Olaroz-Cauchari topographic depression and acts as a barrier between the Olaroz (to the north) and the Cauchari salt pans.

The Cauchari Salar is located at the southern part of the basin, between 23°39′ and 23°50′S, covering an area of ~80 km^2 (Fig. 3B). The dominant lithology in the basin consists of sedimentary sequences and volcanic rocks. The Tocomar River is the major fluvial collector and reaches the salar from the south (Fig. 2). The southern catchment area includes numerous hydrothermal springs.

Shallow brines in both salars are nearly neutral to alkaline, with pH values ranging between 8.10 and 8.50 in Olaroz and from 7.20 to 9.30 in Cauchari (Table 1). The brines´ major chemical composition is dominated by Na/Cl^- type waters (Fig. 4), with TDS values and ionic contents that are up to one order of magnitude higher than those measured in the Jama's brines (from 136,829 to 160,072 mg L^{-1} in Olaroz and from 92,423 to 144,418 mg L^{-1} in Cauchari, Fig. 5). These values represent the highest ionic concentrations measured in the Northern Puna salars. The major ion concentrations in Olaroz's brines are nearly constant across the salt pan surface, while in Cauchari, the highest concentrations are found towards the southern margin.

As observed in the Jama's brines, samples of the Cauchari salar also

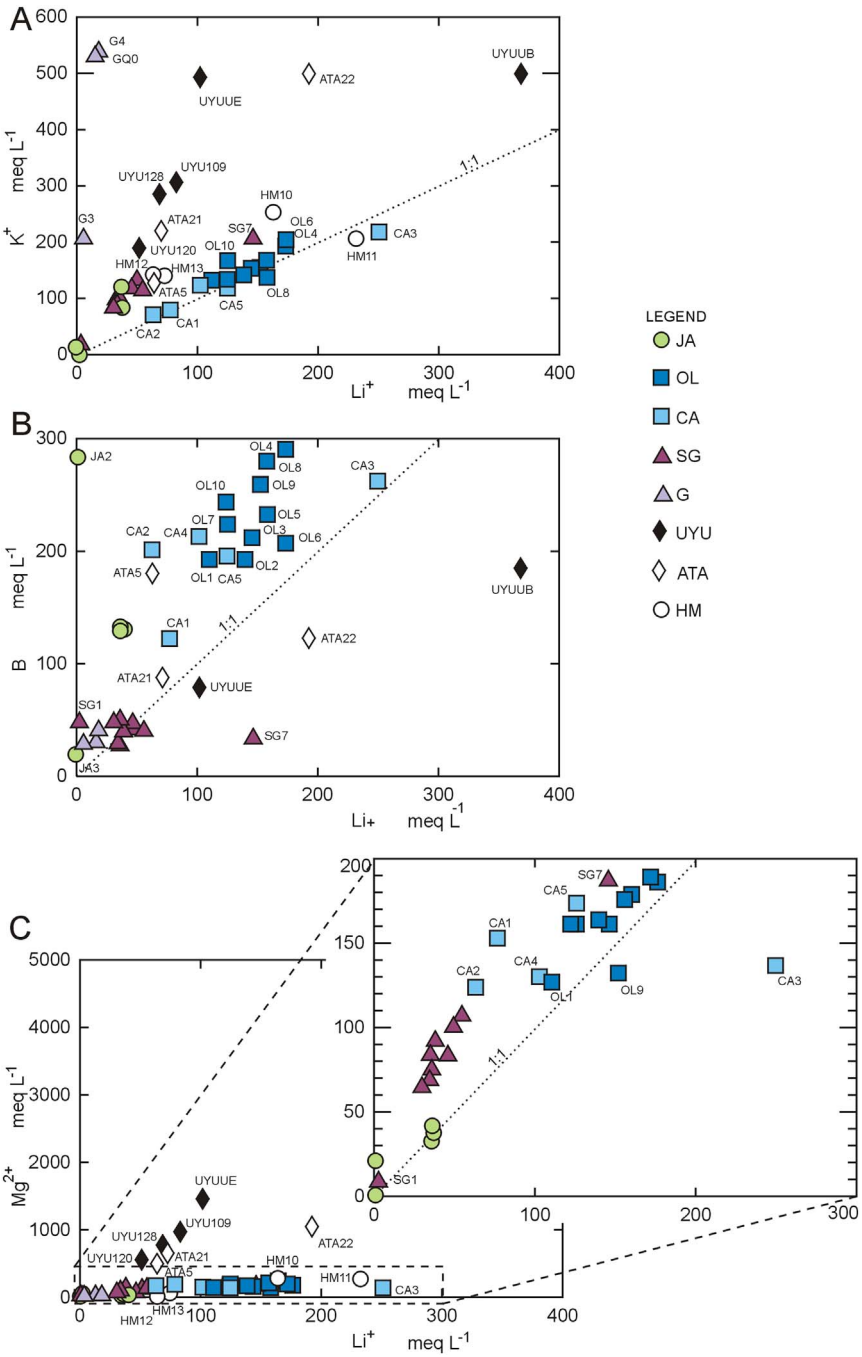

Fig. 7. Scatter diagrams showing the variation of the Li:K ratios (A), the Li:B ratios (B), and the Li:Mg ratios (C). Abbreviations are: Jama (JA), Olaroz (OL), Cauchari (CA), Salinas Grandes (SG), Guayatayoc (G), Hombre Muerto (HM), Uyuni (UYU) and Atacama (ATA). The HM data were taken from Godfrey et al. (2013). The UYU samples UB and UE and the ATA data set are from Risacher and Fritz (2009). The UYU samples 109, 128 and 120 were taken from Ericksen and Salas (1977). The G samples are from López Steinmetz (2017) and samples JA, OL, CA and SG are from this contribution. The HM samples 10, 11 and 12 are lagoon brines, sample 13 is a brine collected at 200 cm depth in a hole drilled into the salar (Godfrey et al., 2013). The UYU samples UB and UE correspond to brines collected at 100 cm depth (Risacher and Fritz, 2009), sample 109 was collected in a brine pool and samples 120 and 128 are brines collected from holes drilled 40 to 50 cm into the salt crust (Ericksen and Salas, 1977). Samples GG_3, GG_4 and GQ_0 were collected from pits dug in the playa lake sediments (López Steinmetz, 2017).

plot along the 1:1 line in Fig. 6A, with a mean Na:Cl ratio of 0.98. The Na:Cl ratios in the Olaroz brines are characterized by $Na^+ < Cl^-$ and a mean ratio of 0.84. The relation between Ca^{2+} and SO_4^{2-} concentrations in Cauchari and Olaroz in the shallowest brines is shown in Fig. 6C. Unlike the Jama's samples, brines of the Olaroz and Cauchari salars do not cluster around the 1:1 line that represents the equilibrium of $CaSO_4$ dissolution, but instead they follow a trend of increasing SO_4^{2-} concentrations at nearly constant Ca^{2+} contents, with $SO_4^{2-} > Ca^{2+}$ in all cases. When considering the relation between Mg^{2+} and SO_4^{2-}, and that of ($Mg^{2+} + Ca^{2+}$) and SO_4^{2-} (Fig. 6E, F) it is observed that samples cluster close to the 1:1 line, which suggests that the dissolution of Ca-Mg sulphate salts may contribute these ions to the water in some parts of these salars. However, the observed general trend is characterized by increasing SO_4^{2-} concentrations at nearly constant Ca^{2+}, Mg^{2+} and ($Ca^{2+} + Mg^{2+}$), which indicates that some other sources are contributing sulphates to the brines. Additional sources could be the non Ca-Mg sulphates (likely Na-sulphates) and/or hydrothermal inputs.

The Li^+ concentration in shallow brines ranges from 771 to 1213 mg L^{-1} in Olaroz and from 442 to1739 mg L^{-1} in Cauchari. The highest Li grade zones occupy the central area of these two salars (Fig. 3B). The mean Li^+ concentration is 860 mg L^{-1} in Cauchari and 1014 mg L^{-1} in Olaroz. The Li concentrations show linear positive trends with K^+ and Mg^{2+}, and the corresponding ratios are characterized by $Li^+ \approx K^+$ and $Li^+ < Mg^{2+}$ (Fig. 7A, C, Table 2). The Li:Mg ratios are 0.86 in Olaroz and 0.89 in the Cauchari brines, while the mean Li:K ratios are 0.92 and 0.99 respectively. The boron concentration in these brines varies between 1336 and 3175 mg L^{-1} (Table 1). Boron do not shows a strict linear correlation with Li contents (Fig. 7B). In all the analysed samples, the concentration of Li is lower

Table 2
Comparative attributes of the Northern Puna's salars and Atacama, Uyuni and Hombre Muerto. The mean Li^+ concentration and Li:Mg ratios of Jama, Olaroz, Cauchari and Salinas Grandes were settled based on original data from this contribution (Table 1). The mean Li^+ concentration and Li:Mg of Guayatayoc correspond to the mean value of the 3 brine samples (samples G3, G4 and Q0) reported in López Steinmetz (2017). The mean Li^+ concentration reported for Atacama are from Ide and Kunasz (1989) and Kunasz (2006), and the mean Li:Mg corresponds to values reported by COCHILCO (2013). The mean Li^+ [a] concentration and Li:Mg [a] ratio in Uyuni corresponds to the mean values of 38 samples (from sample 100 to sample 133 and samples 146, 147 and 147A) reported by Ericksen and Salas (1977). The mean Li^+ [b] concentration and Li:Mg [b] ratio corresponds to the mean values of the 164 samples (from sample UA to sample RZ) reported by Risacher and Fritz (1991). The mean Li^+ [c] concentration and Li:Mg ratio of Hombre Muerto correspond to the mean value of the 9 samples (samples 4, 5, 6 and 9 to 14) reported by Godfrey et al. (2013). The mean Li^+ [d] concentration in Hombre Muerto corresponds to the mean Li^+ concentration of 100 cm-deep brines reported by Garrett (2004) and Kesler et al. (2012).

Salar	Surface (km^2)	Altitude (m a.s.l.)	Mean [Li] ($mg\,L^{-1}$)	Mean [Li:Mg]
Jama	25	4080	82	0.42
Olaroz	130	3903	1014	0.89
Cauchari	80	3903	860	0.86
Salinas Grandes	280	3410	332	0.50
Guayatayoc	140	3400	96	0.92
Atacama	3000	2305	1400	0.16
Uyuni	10,580	3663	316[a]–602[b]	0.07[a]–0.09[b]
Hombre Muerto	300	3970	516[c]–520[d]	0.88

than that of B with a mean Li:B ratio of 0.60 in Cauchari and 0.63 in Olaroz.

4.3. The Salinas Grandes

Salinas Grandes is a large salt pan of 280 km^2 placed at 3410 m a.s.l. between 23°33′–23°45′S and 65°51′–66°12′W (Fig. 3C). This salar is located south of the Las Burras alluvial fan, which separates the Salinas Grandes salt pan from the Guayatayoc playa lake located in the north. Permanent streams feeding the Salinas Grandes include the San Antonio de los Cobres and the El Moreno Rivers. The southern catchment areas, such as the headwaters of the San Antonio de los Cobres River and the Pastos Chicos River include numerous hydrothermal springs (Giordano et al., 2013; Giordano et al., 2016), while the headwater area of the El Moreno basin involves seasonal periglacial processes and relatively large amounts of precipitations (ca. 700 mm/yr) compared with the western part of the basin (ca. 300 mm/yr). The muddy salt shorelines in the mouth of the El Moreno River are mainly developed along the south-eastern border of the salt pan. Quaternary alluvial deposits cover the low lying areas and reach the foot of mountains. The metasedimentary basement and the Cretaceous to Paleocene sedimentary sequences are the most widespread lithologies along the eastern side of the basin, while Paleozoic and Mesozoic plutonic rocks outcrop in the west-boundary ranges.

Similar to the other salars of the study area, shallow brines in the Salinas Grandes are nearly neutral to slightly alkaline, with pH values ranging from 7.10 to 8.00 (Table 1). Salinity shows intermediate values compared with the remaining salars of the Northern Puna, ranging between 11,692 and 120,539 $mg\,L^{-1}$ (Fig. 5B). Major ionic concentrations are dominated by Na and Cl ions (Fig. 4). Interestingly, these brines show the largest variability of the ionic concentrations compared with the neighbour salars (Fig. 5). The Salinas Grandes brines also show nearly equivalent proportions of Ca^{2+}, Mg^{2+} and K^+ with Ca:Mg ~ 1 (Fig. 4). Unlike the other salars of the norther Puna region, the Salinas Grandes' brines typically have $Ca^{2+} > SO_4^{2-}$ ratios. As seen in Fig. 6C, E and F, most samples show a trend of increasing Ca^{2+}, Mg^{2+}, and ($Ca^{2+} + Mg^{2+}$) concentrations at nearly constant sulphate contents, with the exception of samples SG1 located just at the mouth of the El Moreno River, which is nearly one order of magnitude more diluted than the remaining samples collected in the salar. In addition, Ca^{2+} concentrations increase at decreasing $HCO_3^- + CO_3^{2-}$ contents and the same trend is observed with Na^+ concentrations (Fig. 6A, D). Saturation indexes indicate that brines are undersaturated in calcite, aragonite, and dolomite ($SI_{dolomite}$: −2.07 and −1.55, $SI_{aragonite}$: −1.30 to −1.11 and the $SI_{calcite}$: −1.15 and −0.97).

The concentration of boron varies from 309 to 542 $mg\,L^{-1}$, while Li^+ concentrations range between 25 and 1018 $mg\,L^{-1}$. The highest Li grade zone is located in the western margin of the salar, just at the discharge of the San Antonio de los Cobres River (Fig. 3C). The mean Li^+ concentration in the shallowest brines of the Salinas Grandes salt pan is 332 $mg\,L^{-1}$, with a mean Li:K ratio of 0.41 (Fig. 7A), and a mean Li:Mg ratio of 0.50. In all samples, Li concentrations are positively correlated with Ca^{2+}, Mg^{2+} and K^+ concentrations, while they show no correlation with B (Fig. 7).

The concentrations of Li and boron (in $meq\,L^{-1}$; Fig. 7B) involve Li:B > 1 ratios through the western half part of the salt pan (samples SG5, SG6, SG7, SG8, and SG10). These Li > B ratios typically range between 1.10 and 1.32, with the exception of sample SG7 that contains 4.39 times more Li than B. In the central part of the salar, brines contain nearly equivalent proportions of Li and B (samples SG4 and SG9, with Li:B ratios of 0.95 and 0.99, respectively). Brines collected from the easternmost part of the salt pan are characterized by Li:B < 1 (samples SG1, SG2 and SG3, with Li:B ratios of 0.07, 0.67 and 0.70, respectively).

5. Discussion

5.1. Brine types and regional distribution

The major chemical composition of the studied brines is rather constant; brines are typically rich in Na^+ and Cl^-, subordinated SO_4^{2-}, and relatively poor in Ca^{2+}, Mg^{2+} and $HCO_3^- + CO_3^{2-}$. An additional common feature in the Northern Puna brines is that K^+ concentrations are from 2 to 6 times higher than those of Mg^{2+}. Residual brines in Northern Puna salars are characterized by a final major composition dominated by Na^+-Cl^- and SO_4^{2-} ions, which is one typical end member in the chemical divide trend proposed by Hardie and Eugster (1970). According to the Hardie and Eugster model, the major chemical composition of the northern Puna brines is controlled by limited carbonate and Ca^{2+} concentrations that resulted in relative richer contents of sulphate, chloride and sodium at increasing evaporation stages, which is the typical signature of mature brines in equilibrium with halite and mirabilite (Fig. 9).

In the four studied salars, average salinity is the highest in Olaroz and the lowest in Jama, while intermediate values were measured in Cauchari and Salinas Grandes. In addition to salinity, the concentration pattern OL ≥ CA ≥ SG ≥ JA is valid for Mg^{2+}, K^+, Li^+ and B concentrations, but not for Ca^{2+}, whose regional concentration pattern is SG ≥ JA ≥ CA ≥ OL. These trends reveal that brines are more mature along the N-S lineament occupied by the Olaroz-Cauchari salars and less evolved towards the regional margins. The lower Ca^{2+} concentrations observed in Olaroz and Cauchari might be determined by contributions of thermal or freshwaters with depleted Ca^{2+} concentrations and/or it could be the consequence of local geochemical processes that involve precipitation of calcite/aragonite but also of some other Ca-scavenging process such as cation exchange occurring during the interaction of infiltrating water with the reddish and greenish layers of clays accumulated in the salars' sedimentary sequence (López Steinmetz and Galli, 2015). However, the most outstanding feature of these salars is the high Li grades of their brines, with average concentrations from 82 to 1014 $mg\,L^{-1}$, the highest ones found in the Cauchari and Olaroz salt pans.

5.2. The Li concentration patterns

The behaviour of trace elements such as Li and boron in the context of the chemical divide (Hardie and Eugster, 1970) has been scarcely

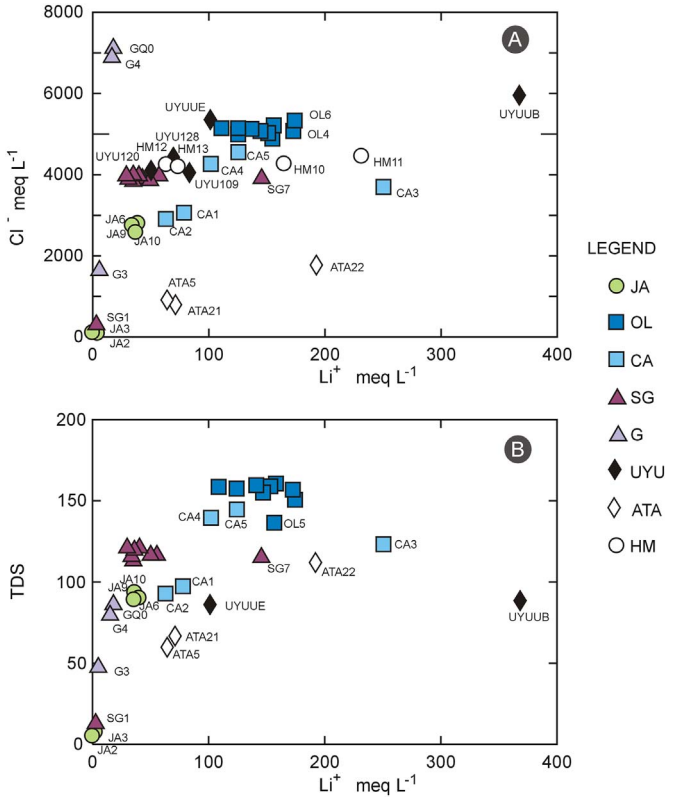

Fig. 8. Scatter diagrams showing the variations of Li^+ versus Cl^- (A) and Li^+ versus salinity (B). Salinity is expressed by TDS (in $g\,L^{-1}$). Jama (JA), Olaroz (OL), Cauchari (CA), Salinas Grandes (SG). Data corresponding to Guayatayoc (G), Hombre Muerto (HM), Uyuni (UYU) and Atacama (ATA) are plotted for comparison. Details concerning the HM, UYU, ATA and G plotted data are presented in caption of Fig. 7.

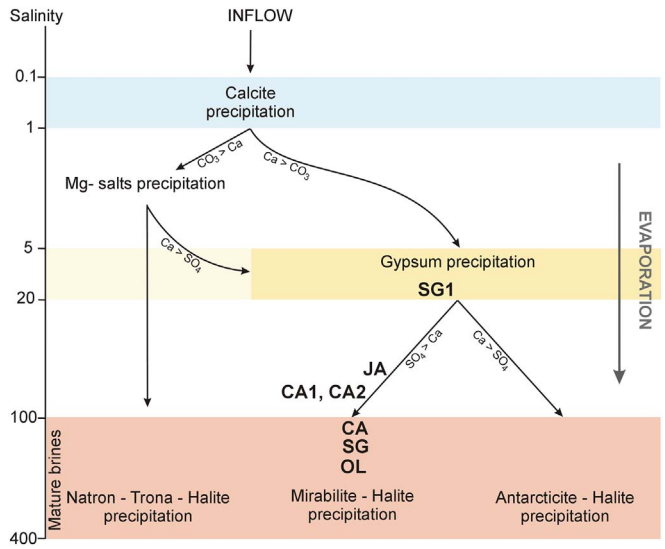

Fig. 9. Flow sheet for evaporative concentration of inflow waters (cf. Hardie and Eugster, 1970, modified from Risacher and Fritz, 2009). Salinity in the left-hand side of the diagram indicates the total dissolved load of the solution in $g\,L^{-1}$. Pathways that resulted in the considered brines are shown with respect to salinity and composition. SG: Salinas Grandes, OL: Olaroz, CA: Cauchari, JA: Jama. The Ca:SO_4 ratios are shown in Fig. 6C.

assessed. For example, Witherow and Lyons (2011) determined on the basis of geochemical modelling that Li is largely conservative in water samples of the Great Basin (USA), Saskatchewan, and the McMurdo Dry Valleys of Antarctica and, thus, its concentration is the result of long-term solute input and concentration through evaporation and/or sublimation processes. According to this, Li behaves as an incompatible element, not only during the stages of magmatic differentiation but also during weathering. Therefore, its concentration during brine evolution should follow an increasing trend with increasing water salinity. However, we have observed no unequivocal correlation between the Li grade of brines and salinity nor other conservative solutes such as Na and Cl (Fig. 8A and B).

Lithium concentrations in the study shallow brines are the result of the balance between inputs from a number of Li-bearing sources and its partial removal by processes acting within the salar's basins. The sources of Li in the studied salt pans are still unknown. However, two types of sources have been the most widely accepted in similar environments: 1) Weathering of Li-bearing minerals present in felsic volcanic rocks such as ignimbrites, and 2) geothermal activity associated with nearby volcanic systems or underlying magmas (Zheng and Liu, 2009; Lowenstein and Risacher, 2009). On the other hand, the removal of Li from water may occur by adsorption onto clay minerals due to the capacity of Li^+ to be incorporated into the mineral interlayers (e.g., Zhang et al., 1998; Williams and Hervig, 2002). The extent of Li scavenging by adsorption onto clay minerals present in the clastic fraction of sediments has not been assessed so far in the northern Puna salars. However, the concentrations of Li determined in the brines, which are from two to three orders of magnitude higher than those measured in rivers discharging into the salars (Franco et al., 2016; Borda et al., 2016; López Steinmetz, 2017), indicate that Li preferentially remains in the solution and concentrates after long-term cycles of water evaporation and precipitation of non Li-bearing soluble salts (e.g., halite). This is supported by the lack of correlation between Li and conservative ions such as Cl^- and Na^+ and the observed trends with salinity. One interesting common feature in the study area is that Li concentrations are positively correlated with K^+ and Mg^{2+}, suggesting a common source for all these ions and similar geochemical behaviour. Local inputs of Li from thermal water contributions is also expected, particularly in Olaroz, Cauchari and Salinas Grandes, where thermal springs have been identified in some parts of the salar complexes (Giordano et al., 2013; Giordano et al., 2016; Peralta Arnold et al., 2017).

5.3. Driving factors on the Li grades

Hydrochemical features of the Andean salars are controlled by a number of variables acting at different scales. In a recent work, Munk et al. (2016) have defined six major features shared by most Li-rich brines deposits at a global scale: (1) arid climate; (2) closed basin containing a salar (salt crust), a salt lake, or both; (3) associated igneous and/or hydrothermal activity; (4) tectonically driven subsidence; (5) suitable Li sources; and (6) sufficient time to concentrate Li in the brine. Even though all these features converge across the Puna Plateau, brines from the studied salars have an uneven distribution of Li grades. Therefore, there must be some key factors controlling the spatial and temporal variability of the Li concentrations in the region.

The hydrothermal activity is considered as one of the most significant factors for the formation of Li and boron rich brines in the Central Andes (Risacher et al., 2003; Godfrey et al., 2013; López Steinmetz, 2017; and references therein). Indeed, a number of authors indicated that the main sources of Li in Uyuni and the nearby salars of Coipasa and Empexa in the southern part of the Bolivian Altiplano are thermal springs associated with Quaternary rhyolitic volcanism (Shcherbakov and Dvorov, 1970; Ericksen and Salas, 1977; Campbell, 2009). Since hydrothermal activity on the region is largely related to volcanism and the formation of the plateau (i.e., Isacks, 1988; de Silva, 1989; Allmendinger et al., 1997; McQuarrie et al., 2002; Kay et al., 2010; Perkins et al., 2016; and references therein), it could be considered that this regionally pervasive and large scale process is most likely a primary condition for the formation of exceptional Li brine-type deposits on the Argentine Puna region.

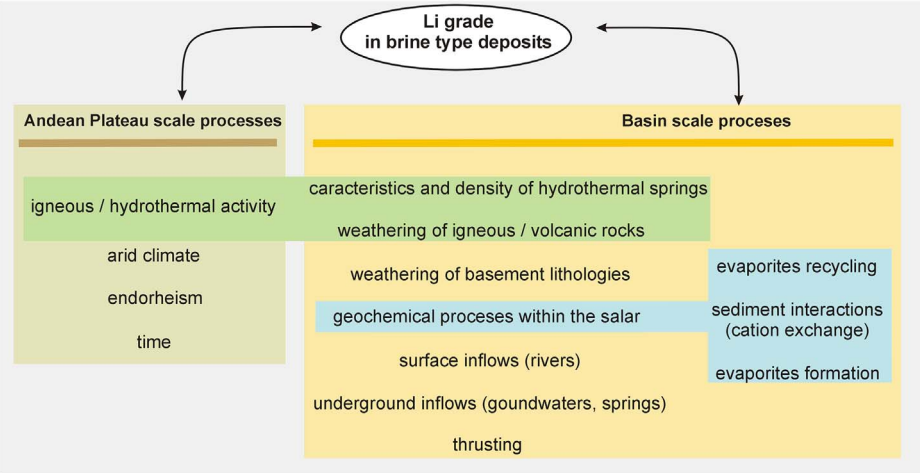

Fig. 10. Model illustration involving the coupled action of basin scale processes and local factors driving the Li grade in evaporative systems from the Andean Plateau.

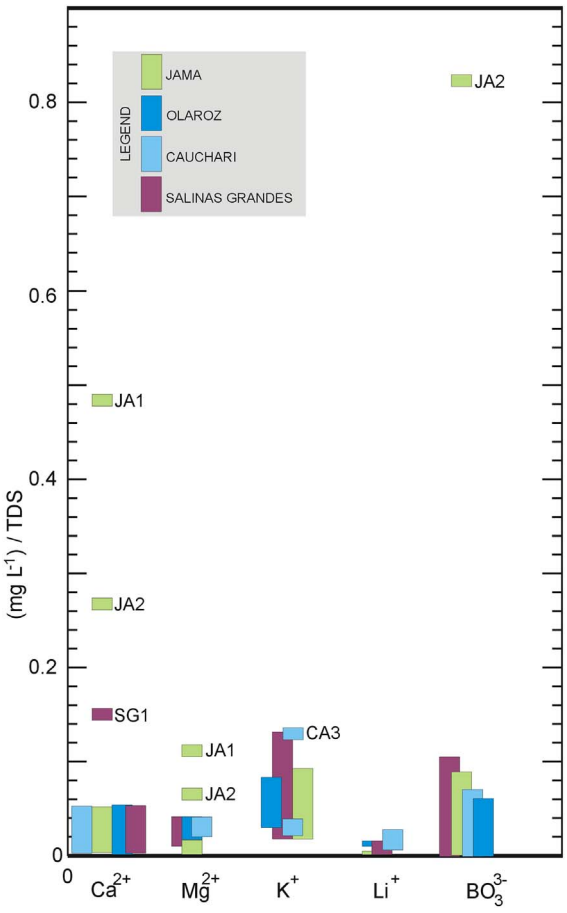

Fig. 11. TDS normalized ionic concentrations in brines from the Salar de Jama (JA), Olaroz (OL), Cauchari (CA) and Salinas Grandes (SG).

The data that we present in this contribution clearly reveal that in the Norther Puna region, the highest concentrations of Li are restricted to the Olaroz and Cauchari salt pans (Fig. 3). These two salars are located in the same tectonically N-S elongated depression. Therefore, the distinctive Li enrichment in Olaroz and Cauchari is being locally influenced by basin-scale processes (Fig. 10), such as the volume and the chemical composition of geothermal waters discharging into the basin, the extent of weathering of Li-rich rocks, and/or geochemical processes taking place within the salars. An additional local factor that may result in increased Li concentrations in the Olaroz and Cauchari's brines should likely be associated to the upflow of hot fluids from the deepest zones of the upper crust throughout major thrusts that enhance the chemical alteration of regional rocks. In the northern part of the Olaroz saline complex, Franco et al. (2016) reported the presence of thermal springs with Li concentrations of ~150 mg L^{-1}. Additionally, the basin involves several hydrothermal fields controlled by deep thrust faults and geographically associated with volcanic centres (Peralta Arnold et al., 2016). High lithium concentrations in mature thermal waters (between 4 and 81 mg L^{-1}) and in those straightly related to dissolution of evaporites (up to 602 mg L^{-1}), coupled with isotopic data ($\delta^{18}O$ and δD) reveal that strong rock interaction processes are likely more significant than the magmatic influence (for details see Peralta Arnold et al., 2017).

The lower Li grade in brines from the Salinas Grandes relative to Olaroz and Cauchari could be associated with some characteristics of the basin: 1) the catchment lithology is dominated by the Eastern Cordillera basement, which is different from that of the Northern Puna, and could, therefore, have a different geochemical signature; and 2) the less arid conditions in the basin's catchments located at the easternmost edge of the Norther Puna region. In the Salinas Grandes, the location of the major fresh inflow (i.e., the El Moreno River) and the Eastern Cordillera basement lithologies are both the geographic factors that prevail east of the salar. This is consistent with the zonation of Li, which decreases towards the southeast (Fig. 3C). On the contrary, throughout the western side of the salar, there are two other factors that may explain the higher Li concentrations: the role of hydrothermalism that is largely represented by the springs that feed the San Antonio de los Cobres River, and the Plateau basement dominant lithology. Consequently, even if the hydrothermal activity - which represents just one of the multiple expressions related to the intrinsic nature of the plateau - is considered as a major source for Li supply, additional geological, climatic, and geochemical aspects locally generating distinctive Li grades and brine compositions in every salt pan and/or basin should also be considered (Fig. 10).

5.4. The boron and potassium signature

In addition to the elevated Li concentrations, the Andean salars´ brines also show high concentrations of B, and K. However, no clear associations have been determined between these ions that could serve to identify parental linkages among them (Fig. 7A, B). As it was previously indicated, Li concentrations show linear positive trends with K concentrations in all the studied salars suggesting common sources and similar geochemical behaviour for these two ions, particularly in Olaroz and Cachauri.

The Li:B ratios in the northern Puna salars (Fig. 7B) involve two

main trends: brines with Li:B > 1, such as those in the western Salinas Grandes, and brines with Li:B < 1 in the remaining cases. Based on B isotopic data, Kaseman et al. (2004) reported two distinctive sources of boron, one associated with volcanic contributions that largely control the formation of borate nodules in salars located westward the Puna plateau, and another one associated with the weathering of the basement rocks that prevail in the easternmost salars. Due to the poor correlation between Li and B concentrations in the studied salars, we cannot certainly extrapolate the Kaseman et al. (2004) conclusions to the Li sources and therefore boron shouldn't be used as a prospective tool for lithium in the region.

5.5. The Li-bearing northern Puna salars in the Andean context

The comparison between the relative abundance of ionic species with respect to the total salinity reveals that the Salinas Grandes brines are proportionally richer in K^+ and B, while the Salar de Cauchari contains proportionally higher Li^+ concentrations than its neighbour Northern Puna salars (Fig. 11). This means that if a brine sample from Cauchari (which is less saline than brines from Olaroz) is hypothetically evaporated in order to increase its salinity up to the values of Olaroz, then, 1 L of the Olaroz brine would have a lower Li grade than the same volume of the Cauchari brine. Consequently, the evaporative concentration process in Cauchari is more efficient than in Olaroz (even if the mean Li^+ concentration of the latter reaches 1014 mg L^{-1} versus 860 mg L^{-1} of the former).

The integrated analysis of the Li-rich brine chemistry from Northern Puna provides important information to evaluate the potentially economic viability of these brines with respect to Li extraction. In addition to the Li grade of brines, the substrate porosity-permeability, the aquifer water balance, and the volume of the host aquifer (Houston et al., 2011), the magnesium content is an additional issue regarding the Li-mining process because Mg^{2+} causes chemical interferences in the brine purification process and limits the Li^+ recovering (e.g., Crespo et al., 1987; An et al., 2012; Kesler et al., 2012; An et al., 2012). The Uyuni's brines typically have high grade Mg^{2+} (Ericksen et al., 1978; Risacher and Fritz, 1991) while the Salar de Hombre Muerto represents the opposite situation, with low magnesium contents (Kesler et al., 2012; Godfrey et al., 2013; Table 2, Fig. 7 C). The Li:Mg ratios in the Northern Puna range from 0.54 to 0.92 (Table 2), which in the regional context make them closer to Hombre Muerto than to Uyuni or Atacama (Fig. 7C). We consider that this pattern could be related to the thickness of the Mesozoic–lower Paleogene sedimentary successions underlying the basin catchments. These sedimentary sequences are characterized by rich Ca and Mg calcareous sandstones and siltstones, whose thickness are larger in the Altiplano than in the Puna Plateau (Rouchy et al., 1993; Sempere et al., 1997; Fink, 2002; Marquillas et al., 2005, among others). Therefore, the weathering of Mesozoic–lower Paleogene rocks would provide larger amount of Mg^{2+} into salt pans in the Altiplano than in the Puna.

Nonetheless, the extremely high Li^+ concentration of Atacama remains the most important difference between all these salars (Table 2). An additional and substantial difference is the oversized surface of Uyuni and Atacama compared with the dimension of the Northern Puna salars. These two aspects, the Li^+ concentration and the salar size, are potentially limiting the whole resources of the Northern Puna salt pans. However, when considering the Li grade and the Li:Mg ratio of brines, the Northern Puna salt pans are revealed as very remarkable Li prospects.

6. Conclusion

This study reports the results of a regional Li exploration campaign covering an area of 9000 km^2 in the Northern Puna that included the four major salars in the region. These evaporite systems represent remarkable Li prospects with mean Li^+ concentrations varying between 82 and 1014 mg L^{-1}, and mean Li:Mg ratios ranging from 0.92 to 0.54.

The major chemical composition of the studied brines is rather constant; most samples are of the Na/Cl^- type with some subordinated samples with a major ionic composition of the Na/Cl^--SO_4^{2-} type, and with K > Mg. Unlike major ions, the concentrations of minor elements such as Mg^{2+}, Li^+ and BO_3^{3-} do not show clear correlation with salinity, which suggest that some other factors are controlling their spatial distribution in the shallowest brines of the studied salars. The absence of a geographical/geomorphological pattern for the ionic concentrations suggests that the hydrochemistry of salars is being partially conditioned by local and regional intrinsic characteristics of each basin, as well as by regional features related to the geological/tectonic nature of the Andean Plateau. These characteristics are likely responsible for the higher Li concentrations in the N-S depression occupied by the Olaroz and Cauchari salars compared with the neighbour salars located towards the margins of the northern Puna region.

Ionic relationships determined in the shallowest brines reveal positive linear correlations between Li, K and Mg, suggesting a common source for these ions. Even though both, Li-rich thermal contributions and the weathering of Li-bearing rocks outcropping in the region are the more likely sources of Li in the norther Puna salars, more comprehensive studies must be conducted in the future in order to better constrain the nature and the extent of contribution from these sources, as well as to define the geochemical/geological mechanisms that control the Li distribution in a regional scale.

The relationship between the Li grade and brine salinity indicates that the evaporative Li recovering should be more efficient in Cauchari than in the remaining salars of the Northern Puna. Despite that the salar dimension is a factor potentially limiting the whole Li resources in the Northern Puna, especially when comparing with Atacama and Uyuni, the Li grade and the Li:Mg ratio in the Northern Puna brines are defining outstanding perspectives for the salt pans of this Andean region.

Acknowledgments

This study was founded by the PRH Red 101 ANPCyT of the Argentine National Government and the National University of Jujuy. R.L. López Steinmetz thanks the grant 2016–2017 and 2018–2019 of the SECTER - UNJu. Other funds came from projects PIO CONICET-UNJu 14020140100010CO, and FONARSEC-FITR Industria 2013 N° 9 (ANPCyT). The laboratory of Aguas de los Andes S. A. provided lab facilities and the Instituto de Geología y Minería (Universidad Nacional de Jujuy) complemented field logistics. The authors thank Ing. Maria Silvina Muhana Senn and Mr. Luis Omar Villegas from Agua de los Andes laboratory for their analytical advising. Special thanks to Captain Christian Meuric for large field logistical support and to the Puna's original inhabitants for their support and hospitality.

Appendix A. Supplementary data

Supplementary data to this article can be found online at https://doi.org/10.1016/j.gexplo.2018.02.013.

References

Allmendinger, W., Jordan, E., Kay, M., Isacks, B.L., 1997. The evolution of the Altiplano-Puna plateau of the Central Andes. Annu. Rev. Earth Planet. Sci. 25, 139–174.
Alonso, R.N., 1986. Ocurrencia, Posición Estratigráfica y Génesis de los Depósitos de Boratos de la Puna Argentina. Universidad Nacional de Salta (PhD Thesis, 196 pp.).
Alonso, H., Risacher, F., 1996. Geoquímica del Salar de Atacama, Parte 1: origen de los componentes y balance salino. Rev. Geol. Chile 23, 127–136.
Alonso, R., Gutiérrez, R., Viramonte, J., 1984. Puna Austral - Bases para el subprovincialismo geológico de la Puna Argentina. In: 9th Congreso Geológico Argentino. vol. 1. pp. 43–63.
An, J.W., Kang, D.J., Tran, K.T., Kim, M.J., Lim, T., Tran, T., 2012. Recovery of lithium from Uyuni salar brine. Hydrometallurgy 117–118, 64–70.
Arias, J., Viera, O., 1982. Estratigrafía y tectónica de la comarca Olacapato - Tuzgle, provincias de Jujuy y Salta, República Argentina. Revista del Instituto de Ciencias Geológicas 5, 71–86 (Jujuy).

Bevacqua, P.S.J., 1992. Geomorfología del Salar de Atacama y estratigrafía de su núcleo y delta, Segunda Región de Antofagasta, Chile. Universidad Católica del Norte, Antofagasta (Undergraduate thesis (unpublished), 284 pp.).
Borda, L.G., Franco, M.G., Córdoba, F., García, M.G., 2016. Geoquímica del Li y As en el salar de Olaroz, Puna de Jujuy. Resultados preliminares. IV Reunión Argentina de Geoquímica de la Superficie (IV RAGSU). Actas de Resúmenes 159.
Boschetti, T., Cortecci, G., Barbieri, M., Mussi, M., 2007. New and past geochemical data on fresh to brine waters of the Salar de Atacama and Andean Altiplano, northern Chile. Geofluids 7, 33–50.
Boutt, D.F., Hynek, S.A., Munk, L.A., Corenthal, L.G., 2016. Rapid recharge of fresh water to the halite-hosted brine aquifer of Salar de Atacama, Chile. Hydrol. Process. 30 (25), 4720–4740.
Campbell, M.G., 2009. Battery lithium could come from geothermal waters. The New Scientist 204 (2738), 23.
Carmona, V., Pueyo, J.J., Taberner, C., Chong, G., Thirlwall, M., 2000. Solute inputs in the Salar de Atacama (N. Chile). J. Geochem. Explor. 69–70, 449–452.
Clesceri, L.S., Greenberg, A.E., Eaton, A.D., 1998. Standard Methods for the Examination of Water and Waste Water, 20th edition. Amer. Public. Health. Assoc., USA.
COCHILCO, 2013. Compilación de informes sobre mercado internacional del litio y el potencial del litio en salares del norte de Chile. http://www.cochilco.cl/estudios/info-litio.asp.
Coira, B., Kay, S., Viramonte, J.G., 1993. Upper Cenozoic magmatic evolution of the Argentine Puna. A model for changing subduction geometry. Int. Geol. Rev. 35, 677–720.
Coira, B., Kay, S., Pérez, B., Woll, B., Hanning, M., Flores, P., 1999. Magmatic sources and tectonic setting of Gondwana margin Ordovician magmas, northern Puna of Argentina and Chile. In: Ramos, V.A., Keppie, D. (Eds.), Laurentia Gondwana Connections Before Pangea. Geological Society of America, Special Paper 336, pp. 145–171.
Coira, B., Caffe, P.J., Ramirez, A., Chayle, W., Diaz, A., Rosas, S., Perez, B., Orozco, O., Marinez, M., 2004. Hoja Geológica 2366-I/2166-III: Mina Pirquitas, Provincia de Jujuy, 1:250,000. Servicio Geológico Minero Argentino, Buenos Aires.
Corenthal, L.G., Boutt, D.F., Hynek, S.A., Munk, L.A., 2016. Regional groundwater flow and accumulation of a massive evaporate deposit at the margin of the Chilean Altiplano. Geophys. Res. Lett. 43 (15), 8017–8025.
Crespo, P., Palma, H., Quintanilla, J., Quispe, L., 1987. Tratamiento químico de salmueras del Salar de Uyuni, Potosí. UMSa-ORSTOM, Informe 7.
Cristiani, C., Del Moro, A., Matteini, M., Mazzuoli, R., Omarini, R., 1999. The magmatism linked to the Jurassic–Cretaceous rift of NW Argentina: the Tusaquillas plutonic complex (Central Andes). In: 14th Congreso Geológico Argentino. 2. pp. 190–193.
Ericksen, G.E., Salas, R., 1977. Geology and resources of salars in the Central Andes. In: U.S. Geological Survey. Open File Repository 88–210 (51 pp.).
Ericksen, G.E., Chong, G., Vila, T., 1976. Lithium resources of salars in the Central Andes. In: Vine, J.D. (Ed.), Lithium Resources and Requirements by the Year 2000. Geological Survey Professional Paper 1005. pp. 66–74.
Ericksen, G.E., Vine, J.D., Ballon, R.A., 1978. Chemical composition and distribution of lithium-rich brines in salar de Uyuni and nearby salars in southwestern Bolivia. Energy 3 (3), 355–363.
Fink, R.J., 2002. Sedimentology and Stratigraphy of the Upper Cretaceous-Paleocene El Molino Formation, Eastern Cordillera and Altiplano, Central Andes, Bolivia: Implications for the Tectonic Development of the Central Andes. Louisiana State University Ph.D. Thesis, 125 pp.
Fornillo, B., Zícari, J., Slipak, A.M., Puente, F., Argento, M., 2015. Geopolítica del litio: industria, ciencia y energía en, Argentina. ed. El Colectivo CLACSO, Buenos Aires (212 pp.).
Franco, M.G., Borda, L., García, M.G., López Steinmetz, R.L., Flores, P., Córdoba, F., 2016. Geochemical and sedimentological characterization of the Salar de Olaroz, northern Argentinean Puna, Central Andes. 3rd International Workshop on Lithium, Industrial Minerals and Energy, Jujuy, Argentina.
Garrett, D.E., 2004. Handbook of Lithium and Natural Calcium Chloride: Their Deposits, Processing, Uses and Properties, 1st edition. Elsevier Academic Press.
Giordano, G., Pinton, A., Cianfarra, P., Baez, W., Chiodi, A., Viramonte, J., Norini, G., Groppelli, G., 2013. Structural control on geothermal circulation in the Cerro Tuzgle-Tocomar geothermal volcanic area (Puna plateau, Argentina). J. Volcanol. Geotherm. Res. 249, 77–94.
Giordano, G., Ahumada, F., Aldega, L., Becchio, R., Bigi, S., Caricchi, C., Chiodi, A., Corrado, S., De Benedetti, A.A., Favetto, A., Filipovich, R., Fusari, A., Groppelli, G., Invernizzi, C., Maffucci, R., Norini, G., Pinton, A., Pomposiello, C., Tassi, F., Taviani, S., Viramonte, J., 2016. Preliminary data on the structure and potential of the Tocomar geothermal field (Puna plateau, Argentina). Energy Procedia 97, 202–209.
Godfrey, L.V., Chan, L.-H., Alonso, R.N., Lowenstein, T.K., McDonough, W.F., Houston, J., Li, J., Bobst, A., Jordan, T.E., 2013. The role of climate in the accumulation of lithium-rich brine in the Central Andes. Appl. Geochem. 38, 92–102.
González, M.A., Tchilinguirian, P., Pereyra, F., Ramallo, E., 2000. Hoja geológica 2366-IV: Ciudad del Libertador General San Martín, 1:250,000. Servicio Geológico Minero Argentino, Buenos Aires.
Gruber, P., Medina, P., 2010. Global Lithium Availability: A Constraint for Electric Vehicles? University of Michigan (Master thesis, 76 pp.).
Hardie, L., Eugster, H., 1970. The evolution of closed-basin brines. In: Fiftieth Anniversary Symposia, Mineralogy and Geochemistry of Non-marine Evaporites. Mineralogical Society of America Special Publication, pp. 273–290.
Houston, J., Butcher, A., Ehren, P., Evans, K., Godfrey, L., 2011. The evaluation of brine prospects and the requirement for modifications to filing standards. Econ. Geol. 106, 1225–1239.
Ide, F., Kunasz, I.A., 1989. Origin of lithium in Salar de Atacama, northern Chile. In: Ericksen, G.E., Cañas Pinochet, M.T., Reinemund, J.A. (Eds.), Geology of the Andes and Its Relation to Hydrocarbon and Mineral Resources. Circum-Pacific Council for Energy and Mineral Resources. Earth Sciences Series, vol. 11. pp. 165–172.
Isacks, B.L., 1988. Uplift of the Central Andean Plateau and bending of the Bolivian Orocline. J. Geophys. Res. 93, 3211–3231.
Jordan, T.E., Mpodozis, C., Munoz, N., Blanco, N., Pananont, P., Gardeweg, M., 2007. Cenozoic subsurface stratigraphy and structure of the Salar de Atacama Basin, northern Chile. J. S. Am. Earth Sci. 23, 122–146.
Kaseman, S.A., Meixner, A., Erzinger, J., Viramonte, J.G., Alonso, R.N., Franz, G., 2004. Boron isotope composition of the geothermal fluids and borate minerals from salar deposits (central Andes/NW Argentina). J. S. Am. Earth Sci. 16, 685–697.
Kay, S.M., Coira, B., Caffe, P.J., Chen, C.-H., 2010. Regional chemical diversity, crustal and mantle sources and evolution of central Andean Puna plateau ignimbrites. J. Volcanol. Geotherm. Res. 198 (1–2), 81–111.
Kesler, S.E., Gruber, P.W., Medina, P.A., Keoleian, G.A., Everson, M.P., Wallington, T.J., 2012. Global lithium resources: relative importance of pegmatites, brine and other deposits. Ore Geol. Rev. 48, 55–69.
King, M., 2010. Amended Inferred Resource Estimation of Lithium and Potassium at the Cauchari and Olaroz Salars Jujuy Province, Argentina. Technical Report. Groundwater Insight, Inc.
Kirschbaum, A., Hongn, F., Menegatti, N., 2006. The Cobres Plutonic Complex, eastern Puna (NW Argentina): petrological and structural constrains for Lower Paleozoic magmatism. J. S. Am. Earth Sci. 21, 252–266.
Kunasz, I.A., 2006. Lithium resources. In: Industrial Minerals and Rocks, Commodities, Markets and Uses, 7th edition. .
López Steinmetz, R.L., 2017. Lithium- and boron-bearing brines in the Central Andes: exploring hydrofacies on the eastern Puna plateau between 23° and 23°30′S. Mineral. Deposita 52, 35–50.
López Steinmetz, R.L., Galli, C.I., 2015. Hydrological change during the Pleistocene-Holocene transition associated with the Last Glacial Maximum-Altithermal in the eastern border of northern Puna. Andean. Geology 42 (1), 1–19.
Lowenstein, T., Risacher, F., 2009. Closed basin brine evolution and the influence of Ca–Cl inflow waters. Death Valley and Bristol Dry Lake, California, QaidamBasin, China, and Salar de Atacama, Chile. Aquat. Geochem. 15, 71–94.
Lupo, L., Morales, M., Maldonado, A., Grosjean, M., 2006. A high-resolution pollen and diatom record from Laguna Los Pululos (22°36′S/66°44′W/4500 m asl), NW Argentinean Puna, since ca. 800 AD. Reconstructing past regional climate variations in South America over the Late Holocene: a new PAGES initiative. In: International Symposium, Malargüe, Argentina. vol. 24.
Maro, G., Caffe, P.J., 2016. The Cerro Bitiche Andesitic Field: pretological diversity and implications for magmatic evolution of mafic centers from the northern Puna. Bull. Volcanol. http://dx.doi.org/10.1007/s00445-016-1039-y. (78-51).
Marquillas, R.A., del Papa, C., Sabino, I.F., 2005. Sedimentary aspects and paleoenvironmental evolution of a rift basin: Salta Group (Cretaceous-Paleocene), northwestern Argentina. Int. J. Earth Sci. 94, 94–113. http://dx.doi.org/10.1007/s00531-004-0443-2.
McGlue, M.M., Ellis, G., Cohen, A., Swarzenski, P., 2012. Playalake sedimentation and organic matter accumulation in an Andean piggyback basin: the recent record from the Cuenca de Pozuelos, NW Argentina. Sedimentology 59, 1237–1256.
McQuarrie, N., Horton, B.K., Zandt, G., Beck, S., DeCelles, P.G., 2002. Lithospheric evolution of the Andean fold-thrust belt, Bolivia, and the origin of the central Andean plateau. Tectonophysics 399. https://doi.org/10.1016/j.tecto.2004.12.013 ((1e4), 15e37).
Méndez, V., Navarini, A., Plaza, D., Viera, O., 1973. Faja Eruptiva de la Puna oriental. In: 5th Congreso Geológico Argentino. 4. pp. 89–100.
Mohr, S., Mudd, G., Giurco, D., 2010. Lithium Resources and Production: A Critical Global Assessment. Prepared for CSIRO Minerals Down Under Flagship, by the Institute for Sustainable Futures, University of Technology, Sydney, and Department of Civil Engineering, Monash University, Final Report. (107 pp.).
Moraga, A., Chong, G., Fortt, M.A., Henríquez, H., 1974. Estudio geológico del Salar de Atacama. Provincia de Antofagasta. Boletín del Instituto de Investigaciones Geológicas. 29 (Santiago, Chile, 56 pp.).
Munk, L.A., Hynek, S.A., Bradley, D., Boutt, D., Labay, K., Jochens, H., 2016. Lithium brines: a global perspective. Rev. Econ. Geol. 18, 339–365.
Orberger, B., Rojas, W., Millot, R., Flehoc, C., 2015. Stable isotopes (Li, O, H) combined with chemistry: powerful tracers for Li origins in Salar deposits from the Puna region, Argentina. Procedia Earth Planet. Sci. 13, 307–311.
del Papa, C., Hongn, F., Powell, J., Payrola, P., Do Campo, M., Strecker, M.R., Petrinovic, I., Schmitt, A.K., Pereyra, R., 2013. Middle Eocene-Oligocene broken foreland evolution in the Andean Calchaquí Valley, NW Argentina: insights from stratigraphic, structural and provenance studies. Basin Res. 25, 574–593.
Peralta Arnold, Y.J., Tassi, F., Caffe, P.J., 2016. Hydrothermal systems and lithium deposits. Northern Puna, Jujuy Argentina. In: 3rd International Workshop on Lithium, Industrial Minerals and Energy, Jujuy, Argentina.
Peralta Arnold, Y.J., Cabssi, J., Tassi, F., Caffe, J.P., Vaselli, O., 2017. Fluid geochemistry of a deep-seated geothermal resource in the Puna plateau (Jujuy Province, Argentina). J. Volcanol. Geotherm. Res. http://dx.doi.org/10.1016/j.jvolgeores.2017.03.030.
Perkins, J.P., Ward, K.M., de Silva, S.L., Zandt, G., Beck, S.L., Finnegan, N.J., 2016. Surface uplift in the Central Andes driven by growth of the Altiplano Puna magma body. Nat. Commun. http://dx.doi.org/10.1038/ncomms13185.
Rettig, S.L., Jones, B.F., Risacher, F., 1980. Geochemical evolution of brines in the Salar de Uyuni, Bolivia. Chem. Geol. 30, 57–79.
Risacher, F., Fritz, B., 1991. Quaternary geochemical evolution of the Salar of Uyuni and Coipasa, Central Altiplano, Bolivia. Chem. Geol. 90, 211–231.
Risacher, F., Fritz, B., 2009. Origin of salt and brine evolution of Bolivian and Chilean Salars. Aquat. Geochem. 15, 123–157.

Risacher, F., Alonso, H., Salazar, C., 1999. Geoquímica de aguas en cuencas cerradas: I, II y III Regiones – Chile. Convenio de Cooperación ORSTOM – DGA – UCN – IRD, SIT 51, Santiago de Chile. (781 pp.).
Risacher, F., Alonso, H., Salazar, C., 2003. The origin of brines and salts in Chilean Salars: a hydrochemical review. Earth Sciences Revue 63, 249–292.
Rouchy, J.M., Camoin, G., Casanova, J., Deconninck, J.F., 1993. The central-Andean basin of Bolivia (Potosí area) during the late Cretaceous and early Tertiary: reconstruction of ancient saline lakes using sedimentological, paleoecological and stable isotopes records. Palaeogeogr. Palaeoclimatol. Palaeoecol. 105, 179–198.
Schmidt, N., 2010. Hydrological and hydrochemical investigations at the Salar de Uyuni (Bolivia) with regard to the extraction of lithium. FOG 26.
Schwab, K., 1973. Die Stratigraphie in der umgebung des salar Cauchari. Geotekt. Forsch., Germany. 43, 168.
Schwab, K., Lippolt, H., 1974. K-Ar mineral ages and Late Cenozoic history of the Salar de Cauchari area (Argentine Puna). In: International Association of Volcanic Chemistry, Earth's Interior Symposium, Andean and Antartic Volcanological Problems, Chile, pp. 698–714.
Seggiaro, R.E., 1994. Petrología, geoquímica y mecanismos de erupción del complejo volcánico Coranzulí (Ph.D. thesis). Universidad Nacional de Salta.
Seggiaro, R.E., 2013. Hoja geológica 2366-III: Susques, 1:250,000. Servicio Geológico Minero Argentino, Buenos Aires.
Sempere, T., Butler, R.F., Richards, D.R., Marshall, L.G., Sharp, W., Swisher, C.C., 1997. Stratigraphy and chronology of Upper Cretaceous-lower Paleogene strata in Bolivia and northwest Argentina. GSA Bull. 109, 709–727.
Shcherbakov, A.V., Dvorov, V.I., 1970. Thermal waters as a source for extraction of chemicals. Geothermics 2 (2), 1636–1639.
de Silva, S.L., 1989. Altiplano-Puna volcanic complex of the Central Andes. Geology 17, 1102–1106.
Soler, M.M., Caffe, P.J., Coira, B.L., Onoe, A.T., Kay, S.M., 2007. Geology of the Vilama caldera: a new interpretation of a large scale explosive event in the Central Andean plateau during the Upper Miocene. J. Volcanol. Geotherm. Res. 164, 27–53.
Stoertz, G.E., Ericksen, G.E., 1974. Geology of salars in northern Chile. Geol. Surv. Prof. Pap. 811 (65 pp.).
Turner, J.C., 1959. Estratigrafía del Cordón de Escaya y la Sierra de Rinconada, Jujuy. Rev. Asoc. Geol. Argent. 15 (1), 15–39.
Turner, J.C., 1960a. Estratigrafía de la Sierra de Santa Victoria y adyacencias. Boletín de la Academia Nacional de Ciencias. 41 (2), 163–169 (Córdoba).
Turner, J.C., 1960b. Estratigrafía del Nevado de Cachi y sector al oeste (Salta). Acta Geológica Lilloana. 3, 191–226.
Turner, J.C., 1972. Puna. Geología Regional Argentina. 1, 13–56 (Buenos Aires).
Warren, J.K., 2010. Evaporites through time: tectonic, climatic and eustatic controls in marine and nonmarine deposits. Earth Sci. Rev. 98 (3), 217–268.
Williams, L.B., Hervig, R.L., 2002. Exploring intracrystalline boron isotope variations in mixed-layer illite/smectite. Am. Mineral. 87.
Witherow, R.A., Lyons, W.B., 2011. The fate of minor alkali elements in the chemical evolution of salt lakes. Saline Systems 7 (2), 2–14.
Yaksic, A., Tilton, J.E., 2009. Using the cumulative availability curve to assess the threat of mineral depletion: the case of lithium. Res. Policy 34, 185–194.
Zappettini, E., 1989. Geología y metalogénesis de la región comprendida entre las localidades de Santa Ana y Cobres, Provincias de Jujuy y Salta. República Argentina. Universidad de Buenos Aires (Ph.D. thesis, 189 pp.).
Zhang, L., Chan, L.H., Gieskes, J.M., 1998. Lithium isotope geochemistry of pore waters, ocean drilling program sites 918 and 919, Irminger Basin. Geochim. Cosmochim. Acta 62.
Zheng, M., Liu, X., 2009. Hydrochemistry of salt lakes of the Qinghai-Tibet Plateau, China. Aquat. Geochem. 15.